Pergamon

PII: S0191-8141(97)00004-7

Journal of Structural Geology, Vol. 19, No. 6, pp. 799 to 815, 1997

0191-8141/97 $17.00 + 0.00

Characteristics and occurrence of bedding-parallel slip surfaces and laminated veins in chevron folds from the Bendigo–Castlemaine goldfields: implications for flexural-slip folding

T. J. FOWLER

Geology Department, School of Science and Engineering, La Trobe University, Bendigo P.O. Box 199, Bendigo, Victoria 3550, Australia

and

C. N. WINSOR*

Mineral Resources, School of Engineering, University of South Australia, The Levels, SA 5095, Australia

(*Received* 27 *June* 1996; *accepted in revised form* 4 *January* 1997)

Abstract—The occurrence of bedding slip planes and associated slip-striated, laminated, quartz veins in the Bendigo–Castlemaine goldfields, southeastern Australia was investigated. Bedding slip planes are concentrated in thin siltstone layers. Data from surface stratigraphic sections on the limbs of five major anticlines gave a mean slip-plane spacing of 8.9 m ($N = 96$), and a mean laminated vein thickness of 19 mm. Most laminated veins are < 20 mm thick and discontinuous along strike and around fold hinges; thicker veins are correspondingly more continuous and are traceable around fold hinges. The mean thickness of laminated veins from individual fold limbs increases with increasing mean spacing of slip planes on each limb, suggesting a sympathetic relationship between vein thickness and net slip; however, there is no such correlation between individual vein thickness and spacing. These relations are explained using a model for the progressive generation of bedding slip planes via shear failure at competent–incompetent layer interfaces as a result of shear strain rate incompatibilities between competent and incompetent beds during fold limb steepening. The model predicts flexural-slip activity continuing well into the stage of homogeneous flattening of the folds, and gives rise to a population of slip planes dominated by those with low net slip. © 1997 Elsevier Science Ltd

INTRODUCTION

Flexural-slip folding is commonly associated with the development of natural chevron folds and plays an essential role in the formation of parallel folds in thinly bedded sequences lacking thick incompetent interlayers (de Sitter, 1958; Ramsay, 1967, p. 391; Hills, 1972, p. 233; Ramsay and Huber, 1987, p. 445; Tanner, 1989). The activity of the flexural-slip process during fold amplification in sequences of thinly bedded alternating competent and incompetent layers has been investigated in natural examples (Chappell and Spang, 1974; Boulter, 1979; Tanner, 1989, 1992), and in laboratory experiments (Ghosh, 1968; Cobbold *et al.*, 1971; Honea and Johnson, 1976; Behzadi and Dubey, 1980). Johnson and Honea (1975) were successful in generating chevron folds in viscous multilayers with welded interlayer contacts, and therefore concluded that interlayer slip is apparently not essential in the attainment of chevron fold shapes. However, interlayer slip strongly influences the characteristics of fold growth, for example the rate of fold amplification relative to bulk shortening (Johnson and Pfaff, 1989). These results suggest that future attempts to understand the significance of flexural-slip folding should not assume from the outset that ready slip can occur on all interlayer surfaces.

The spacing of bedding slip planes (including those bedding-parallel laminated veins that are slip generated) is known to be variable (Tanner, 1989), however few investigators have attempted to clarify the controls on slip-plane spacing and activity during folding (e.g. Chappell and Spang, 1974; Behzadi and Dubey, 1980; Tanner, 1989, 1992). Quantities such as the bedding slip-plane dimensions, spacing and net slip are relevant data assisting the understanding of the role of flexural-slip folding in natural chevron folds. Unfortunately net slip on bedding planes is particularly difficult to measure owing to the rarity of displacement indicators which are pre-folding and discordant to bedding (e.g. clastic dykes), although Tanner (1992) noted that the relative thickness of laminated veins was a reasonably good indicator of the amount of net slip on bedding planes.

Identifying the differences between pre-folding and synfolding bedding-parallel laminated veins is the subject of ongoing debate. Graves and Zentilli (1982), Fitches *et al.* (1986), Henderson *et al.* (1990), Cosgrove (1993) and Jessell *et al.* (1994) have argued for a general pre-folding origin for laminated veins on the basis that: the veins are folded and overprinted by axial-plane cleavages; show

*Author to whom correspondence should be addressed.

extreme variability in vein wall slip-striation orientations; show apparent vein opening directions incompatible with (indeed reverse to) those expected for dilating slip surfaces during flexural-slip folding; and are sometimes composed of quartz columns orientated normal to the vein wall. Keppie (1976), Mawer (1987) and Tanner (1989) regarded the laminated veins as typically synfolding, and directly related to flexural-slip activity along bedding planes. Tanner (1989) found that net slip on bedding-parallel laminated veins on the limbs of chevron folds in the Cornwall area was sufficient to account for the increased limb dips by the flexural-slip mechanism. Other evidence for a synfolding origin of these veins includes a systematic reversal of the sense of shear on opposite fold limbs shown by shear fibre steps on the veins (in a sense which is compatible with flexural-slip folding; Tanner, 1989), vein wall slip lineations lying statistically normal to local fold hinges and the dying out of laminated veins as fold hinges are approached. Of course, it is possible that both pre- and synfolding models are applicable to nature, and there may be a continuity of veins from pre-folding to synfolding stages, as was suggested by Tanner (1990).

The chevron-folded turbidites of the Bendigo–Castlemaine goldfields of southeastern Australia preserve abundant evidence for slip on bedding-parallel laminated veins (Fig. 1). The slip-lineation orientations lie statistically normal to the local fold hinges, although there are some large angular deviations from this relationship in individual cases. A recent microstructural study of these veins (Fowler, 1996) has concluded that the majority have formed during or after the development of a crenulation cleavage in the country rock slate. The opening of the veins involves shear displacement across the vein walls with a shear sense invariably compatible with that required by flexural-slip folding. Therefore, for the Bendigo–Castlemaine region we regard these veins to have a synfolding origin.

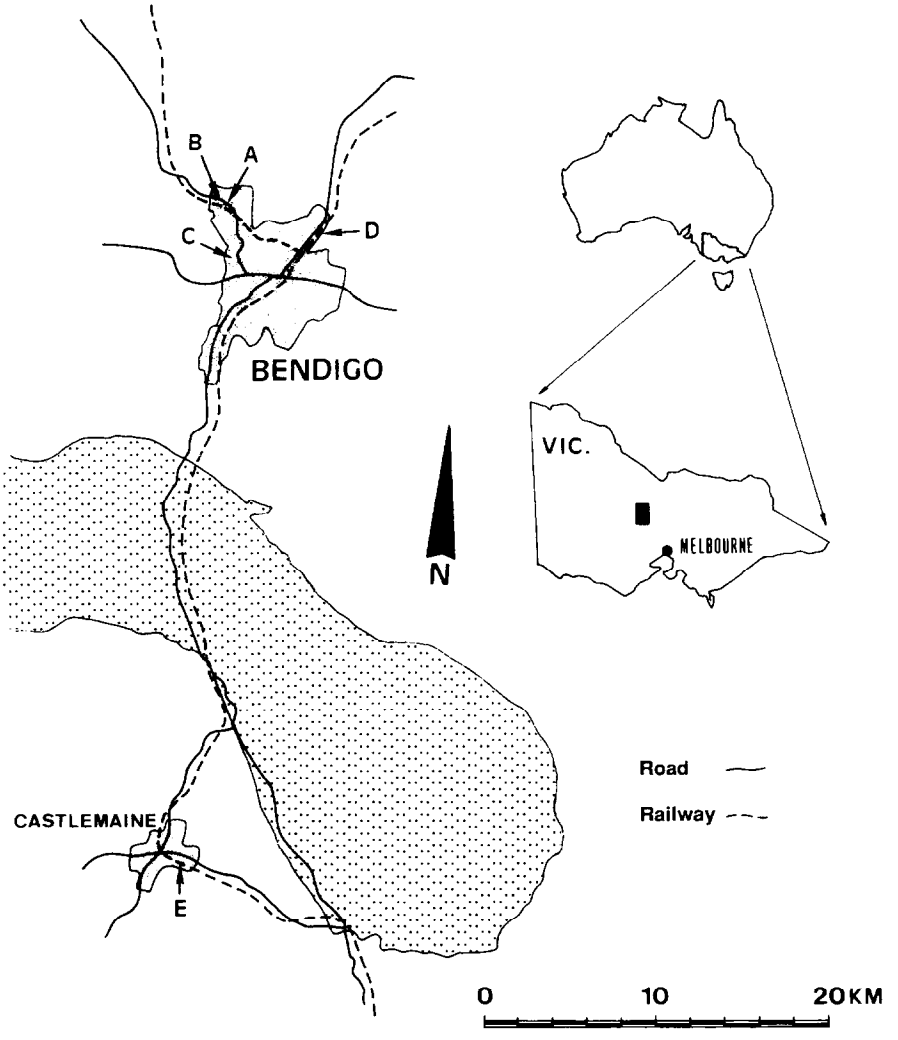

Fig. 1. Map showing the location of the Bendigo–Castlemaine goldfields area in Victoria, Australia. The area of paired-dot ornament represents the Late Devonian Harcourt Granodiorite. The location of the five surface sections from which bedding slip-plane and laminated vein data were collected are also shown: A, Eaglehawk railway cutting (eastern limb of the Derby Anticline); B, Eaglehawk railway cutting (western limb of the Garden Gully Anticline); C, Victoria Hill (eastern limb of the New Chum Anticline); D, White Hills (western limb of the Apollo Anticline); and E, Castlemaine railway cutting (unnamed anticline, 1 km east of Castlemaine). For precise locations of the sections, see Table 1.

Table 1. The five stratigraphical sections forming the dataset

Location*	Figure reference	Anticline	Fold limb	Stratigraphic thickness† (m)	Ordovician stage‡
Eaglehawk[1]	Fig. 1, location A	Derby	Eastern	148	Be3, Be4, Ch1
Eaglehawk[2]	Fig. 1, location B	Garden Gully	Western	166	Be4, Ch1, Ch2
Victoria Hill[3]	Fig. 1, location C	New Chum	Eastern (part)	56	Be4, Be4
White Hills[4]	Fig. 1, location D	Apollo	Western (part) 258	258	Be1
Castlemaine[5]	Fig. 1, location E	Unnamed	Eastern (part)	714	Ca1
Castlemaine[5]	Fig. 1, location E	Unnamed	Western (part)	153	Ca1, Ca2

*Location: [1]GR 5470 3225 (7724 1 Huntley 1:50,000 Topographic Map). Section begins at the GR and extends 400 m southeast; [2]GR 5412 3270 (7724 4 Raywood 1:50,000 Topographic Map). Section begins at the GR and extends 210 m west-northwest; [3]GR 5520 2865 (7724 2 Bendigo 1:50,000 Topographic Map). Section begins at the GR and extends 100 m northeast; [4]GR 5930 3065 (7724 1 Huntley 1:50,000 Topographic Map). Section begins at the GR and extends 280 m southwest; [5]GR 5319 9316 (7723-4-1 Castlemaine 1:25,000 Topographic Map). The eastern limb section begins at the GR and extends 120 m east. The western limb section begins at the GR and extends 140 m west. All maps are available from the Division of Survey and Mapping, Department of Crown Lands and Survey, Melbourne 3002, Australia.

†This refers to the measured stratigraphic thickness (in m) which is continuously exposed in each section.

‡The stages of the Victorian Ordovician, which are relevant to these sections, are (in order of decreasing age) the Castlemainian (Ca), Bendigonian (Be) and Chewtonian (Ch), with substages referred to as, for example, Ca1, Ca2, etc.

This contribution presents data on the lithological controls, spacing, thickness, continuity and orientation of the bedding slip planes, laminated veins and slip lineations from the limbs of five major chevron folds in the Bendigo–Castlemaine goldfields. The data have been collected from measured complete stratigraphic sections and mapped continuous outcrops, and are compared with data from subsurface mine sections. Vein microstructures from these rocks have been reported by Cox (1987), Jessell *et al.* (1994) and Fowler (1996). The implications of these data for flexural-slip activity during fold amplification are evaluated with the assistance of a computer simulation of slip-plane generation via shear failure.

Identification of bedding-parallel slip planes

Bedding slip planes were identified as those showing: (1) bedding-parallel laminated veins or veins with consistently inclined fibres; and/or (2) striated (usually slickensided) bedding surfaces. Close inspection of bedding surfaces was assisted by the obliquity of beds in railway sections, leading to step-like breakages along and across beds. There are rare non-laminated bedding-parallel veins, lacking fibres or striated walls and filled with milky vein quartz, and these were excluded from the dataset.

GEOLOGICAL SETTING

The chevron folds of the Bendigo–Castlemaine goldfields are developed in a 2000+ m thick sequence of Lower Ordovician turbiditic quartz-rich sandstones and siltstones, which were deformed during an E–W compression event (Gray, 1988; Ramsay and Willman, 1988; Gray and Willman, 1991), recently dated as Silurian (440–420 Ma) by Bucher *et al.* (1996). The folds have upright to steeply (75°E–80°W) inclined N- to N15°W-trending axial planes and have gentle (<25°) northerly- and southerly-plunging fold hinges. The fold traces are gently sinuous and continuous for tens of kilometres along trend, have wavelengths of 200–300 m, and a typical interlimb angle of 40°. Details of the geology of the Bendigo and Castlemaine goldfields are reported in Stone (1937), Thomas (1953), Willman (1988) and Cox *et al.* (1991).

Location of areas for data collection

Five stratigraphic sections were chosen for their continuous outcrop and the absence of significant faulting. The sections cover a range of stratigraphic positions within the thick Ordovician sequence, and include Castlemainian (Ca), Bendigonian (Be) and Chewtonian (Ch) stages (Table 1). Their locations and stratigraphic thicknesses are also presented in Table 1. Each section begins at an anticlinal axial plane. Data on the stratigraphic setting, spacing and continuity of slip surfaces, laminated vein thickness, slip lineation orientations, etc., from these sections are presented below and compared with reported data from detailed mine sections.

RESULTS

Stratigraphic spacing of slip planes

The total number of laminated veins and bedding slip planes examined from surface stratigraphic sections was 96, giving a mean stratigraphic spacing between slip planes of 8.9 m for the Bendigo–Castlemaine region. Since we cannot be certain that every slip plane has been identified, this mean spacing value must be considered as a maximum value. Table 2 compares spacing statistics for bedding slip planes determined in this study with data from Jessell *et al.* (1994) and from underground mine sections.

Apart from the variation in the range of mean spacings amongst the five folds surveyed, the present study confirms the estimates made by Jessell *et al.* (1994) that were based on detailed mine sections. However, our estimate of overall mean spacing from examination of surface sections is about 30% lower than that determined

Table 2. Stratigraphical spacing of bedding slip planes

	Mean spacing range* (m)	Mean spacing† (m)	Range of maximum intervals‡ (m)
This study	3.5–11.7	8.9	14.3–52.8
Mine sections	10–19	13.0	12–50
Jessell *et al.* (1994)	4–15	13.2	

*'Mean spacing range' represents the range of values of mean spacing (in m) on individual fold limbs and in individual mine sections.
†'Mean spacing' is the mean bedding slip-plane spacing (in m) for all the data.
‡'Range of maximum intervals' is the range of the greatest thicknesses of slip plane free strata from section to section (in m).

from mine sections. It is likely that the thinnest veins and some individual slip planes were not identified in the mine surveys, which were conducted under poor lighting conditions in the early part of this century. This conclusion is consistent with the upper limit of our mean spacing ranges being lower than those determined from mine survey data.

A histogram showing frequencies for 0.5 m slip-plane spacing class intervals is presented in Fig. 2(a), which shows that closely-spaced slip surfaces predominate. There is a gradual increase in the proportion of closer-spaced slip planes. More than half of the slip planes were found closer than 3.0 m from the next slip plane above. A histogram of spacings to the nearest-neighbour slip plane (Fig. 2b) emphasizes the predominance of the close spacings, and reflects the common tendency for bedding slip planes to occur in close-spaced pairs or clusters (Fig. 3). However, no duplex structures, such as those described by Tanner (1992), were identified. The histograms in Fig. 2 are markedly different from the corresponding histogram for laminated vein spacing presented by Jessell *et al.* (1994, fig. 7a) which was based on data from subsurface mine sections. In particular, their 0–5 m spacing interval represents only 12% of the dataset. Again this is likely to be due to the omission of thinner laminated veins in the underground surveys forming the Jessell *et al.* (1994) dataset.

Stratigraphic and sedimentological controls

Examined stratigraphic sections were divided into the four facies defined by Cas *et al.* (1983) for the

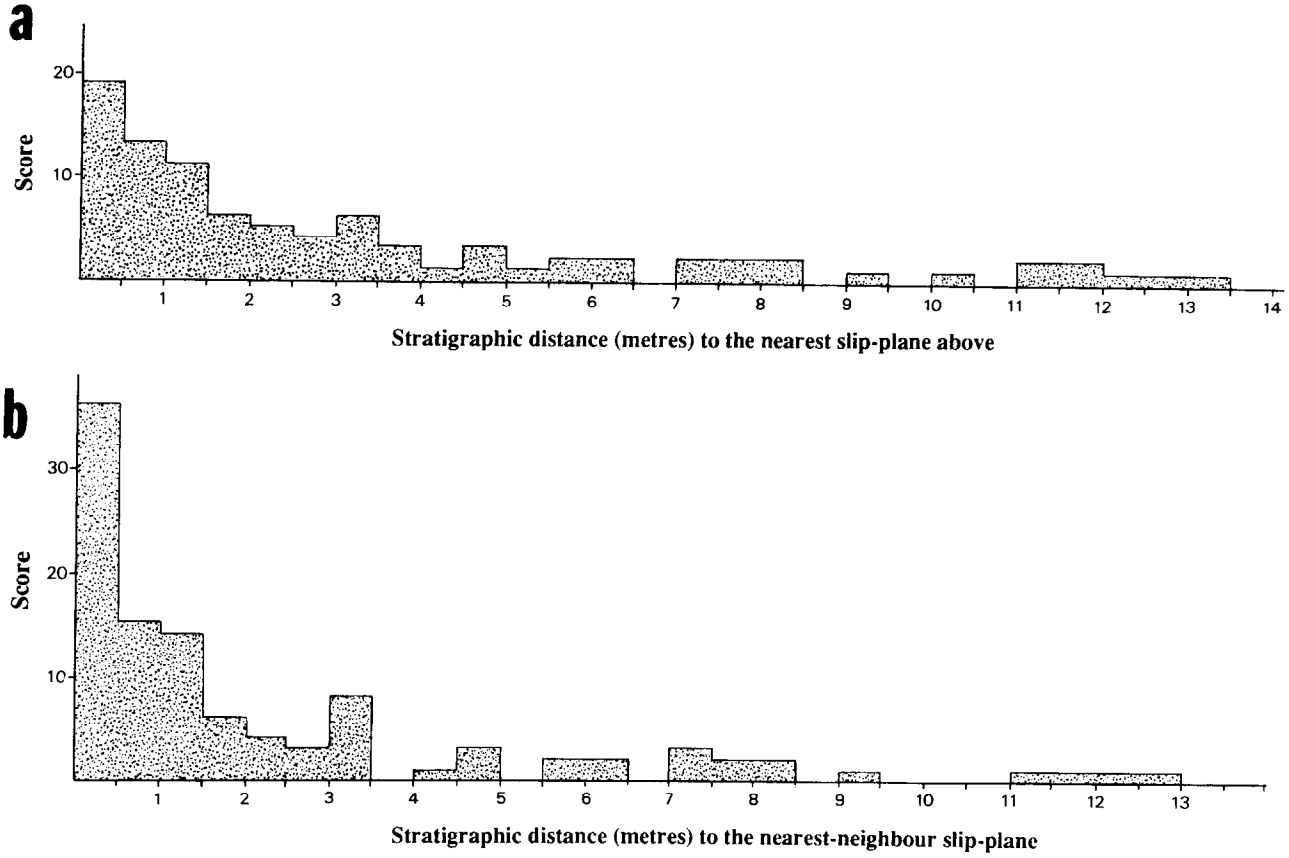

Fig. 2. (a) Histogram of frequencies for 0.5 m bedding slip-plane spacing class intervals representing distance to the nearest slip plane stratigraphically above (data from all measured sections). (b) Histogram of 0.5 m bedding slip-plane spacing class intervals to nearest-neighbour slip planes (data from all measured sections).

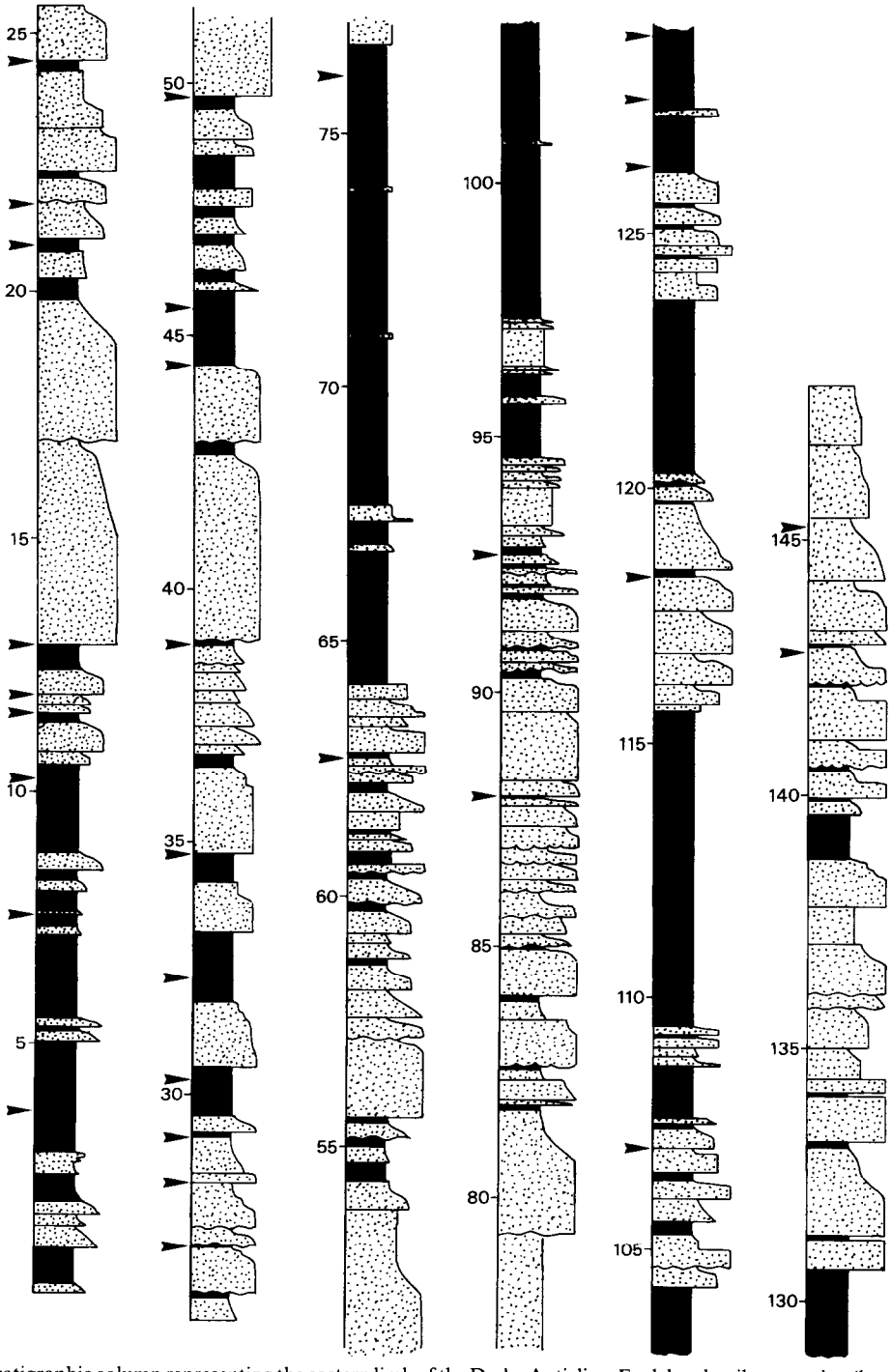

Fig. 3. Stratigraphic column representing the eastern limb of the Derby Anticline, Eaglehawk railway cutting (location A, Fig. 1), showing the sedimentological control on the location of bedding slip-planes (represented by arrowheads). Numbers are metres of stratigraphic thickness measured from the outcrop of the anticlinal axial plane. Stippled beds are sandstones. Dark beds are siltstones.

Castlemaine Supergroup, in order to see if facies influenced the location of bedding slip planes. The four facies are: (1) the *sandstone facies* (amalgamated thick sandstones with frequent Bouma *a* horizons and a sand:mud ratio >6:1); (2) the *sandstone-dominant facies* (thick sandstones, common Bouma *a–c–e* sequence and a sand:mud ratio between 3.5:1 and 6:1): (3) the *mixed sandstone–mudstone facies* (thinly interbedded sandstone and mudstone with common Bouma *b–c–d* sequence and sand:mud ratios between 0.5:1 and 3.5:1); and (4) the *mudstone-dominant facies* (thick mudstone intervals with a sand:mud ratio <0.5:1). The results are presented in Table 3.

Overall the occurrence of bedding slip planes is not influenced by either of the two main facies (sandstone facies and mudstone-dominant facies). There are fewer

Table 3. Proportions of the four sedimentary facies (of Cas *et al.*, 1983) and frequency of bedding slip planes in each facies

Facies	Percentage of total section	Percentage of total bedding slip planes
1. Sandstone	25.4	28.1
2. Sandstone dominant	13.0	1.6
3. Mixed sandstone–mudstone	9.9	17.2
4. Mudstone dominant	51.7	53.1

examples of bedding slip planes in the sandstone-dominant facies and more in the mixed sandstone–mudstone facies than would be expected according to their contribution to the sections. This may be related to an element of subjectivity in locating boundaries of facies 2 and 3. Bedding slip planes were commonly located at the boundaries between facies, particularly at the boundaries of sandstone facies. Eight of the 10 identified boundaries (stratigraphically higher or lower) between the sandstone facies and any other facies were occupied by a bedding-parallel slip plane. This is probably due to the unusual thickness and shear strength of the sandstone facies units, and the magnitude of the competence contrast at these boundaries, favouring shear failure.

On the exposure scale, primary structures clearly exert control on the detailed location of the slip planes. This is evident in the stratigraphic column shown in Fig. 3. Including data for all measured surface sections, 67% of bedding slip planes were entirely within siltstone beds, 8% were located in graded sandstone beds (but always towards the fine-grained top of these beds) and 25% were located along the contact between a sandstone and a siltstone bed. The latter slip planes were three times more likely to be located at the sharp contact between a siltstone and the overlying sandstone than along the gradational contact between a sandstone and the overlying siltstone. Of all the bedding slip planes identified, about 40% lay in siltstones within 10 cm of the base of an overlying sandstone bed. This 10 cm range corresponds to the observed amplitude of bedding sole structures such as scours and load casts. Very similar observations to these have been reported by Tanner (1989).

As 92% of all bedding slip planes were located within siltstones or at their contact with sandstone beds, the thicknesses of siltstone beds that contain slip planes was investigated to determine whether siltstone bed thickness was a controlling factor on slip-plane localization. According to the model for chevron folding devised by Ramsay (1974), the thickness of incompetent layers may vary on chevron fold limbs without destabilizing the fold structure. Ramsay calculated that for any limb dip, A, the amount of shear strain imposed on the incompetent beds is $\tan A + (\tan A - A)t_1/t_2$, where t_1 and t_2 are the competent and incompetent layer thicknesses, respectively. This model suggests that at any limb dip, shear

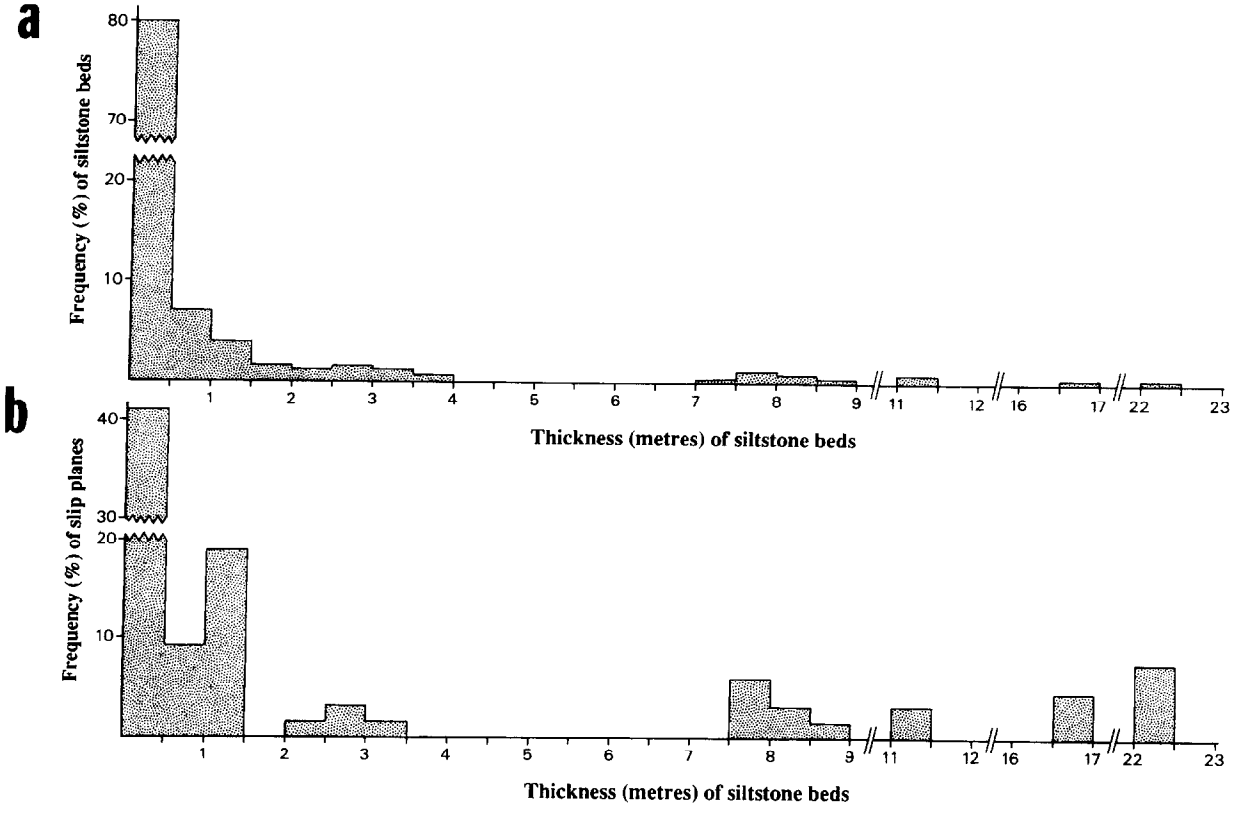

Fig. 4. (a) Histogram of the frequency of 0.5 m thickness class intervals for siltstone beds (data from all measured sections). (b) Histogram of the frequency of occurrence of bedding slip planes in each thickness class interval of (a).

strains rise most rapidly in the thinnest incompetent beds. The Ramsay (1974) model, strictly speaking, is valid only if competent layer thicknesses are constant. Limb-dip incompatibilities are liable to arise from thickness variations in the competent layers, however such limb-dip incompatibilities are insignificant when the ratio t_1/l is of the order of magnitude of 0.01 (Ramsay, 1974, fig. 5), where l is the fold limb length. In the Bendigo–Castlemaine folds t_1/l does not exceed 0.02 (Fowler and Winsor, 1996).

If shear strain rate during limb steepening is a controlling factor in the initiation of slip on bedding, then in the simplest analysis, one would expect slip planes to be concentrated in the thinnest incompetent beds. A histogram showing the distribution of thicknesses of siltstone beds for all measured sections is presented in Fig. 4(a). Nearly 80% of siltstone beds are 0–0.5 m thick, and the frequency of beds drops rapidly as thicknesses increase. Figure 4(b) shows that 41% of slip planes occur in the 0–0.5 m thickness range. For thicker class intervals, frequencies in Fig. 4(a & b) do not correlate well. However, altogether only 10% of siltstone beds in the <0.5 m thickness range were hosts to bedding slip planes. This is compared to 22% of beds in the 0.5–1.0 m range and 62% of beds in the 1–1.5 m range. Beyond these ranges of thicknesses the number of examples is too small for confidence. The under-representation of slip planes in the thinnest siltstones is likely to be due to the marked discontinuous nature of these beds observed along strike. The thinnest continuous siltstone units are in the range 1–1.5 m, and these have the highest proportion of bedding slip planes.

Orientation of slip striations on bedding slip planes

The orientation of slip lineations from the Apollo Anticline, Derby Anticline and the unnamed anticline located 1 km east of Castlemaine (locations on Fig. 1) are presented on stereograms and lineation pitch histograms in Fig. 5. The stereogram of slip-lineation orientations for the above three anticlines (Fig. 5a) demonstrates that these lineations scatter around a mean pitch angle that is orthogonal to the local fold-axis orientation or lies within 5° of being so. Our data suggested that for all of the anticlines studied, 80–95% of the slip lineations lie within 20° (pitch) of being orthogonal to the local fold axis.

On Fig. 5(a) slip lineations measured on the same laminated vein but on different laminae within that vein are shown connected by great circle arcs. Within a single vein, slip-lineation pitch variations of 10° are common, pitch differences greater than 40° are rare, but variations exceeding 60° have been recorded. On the eastern limb of

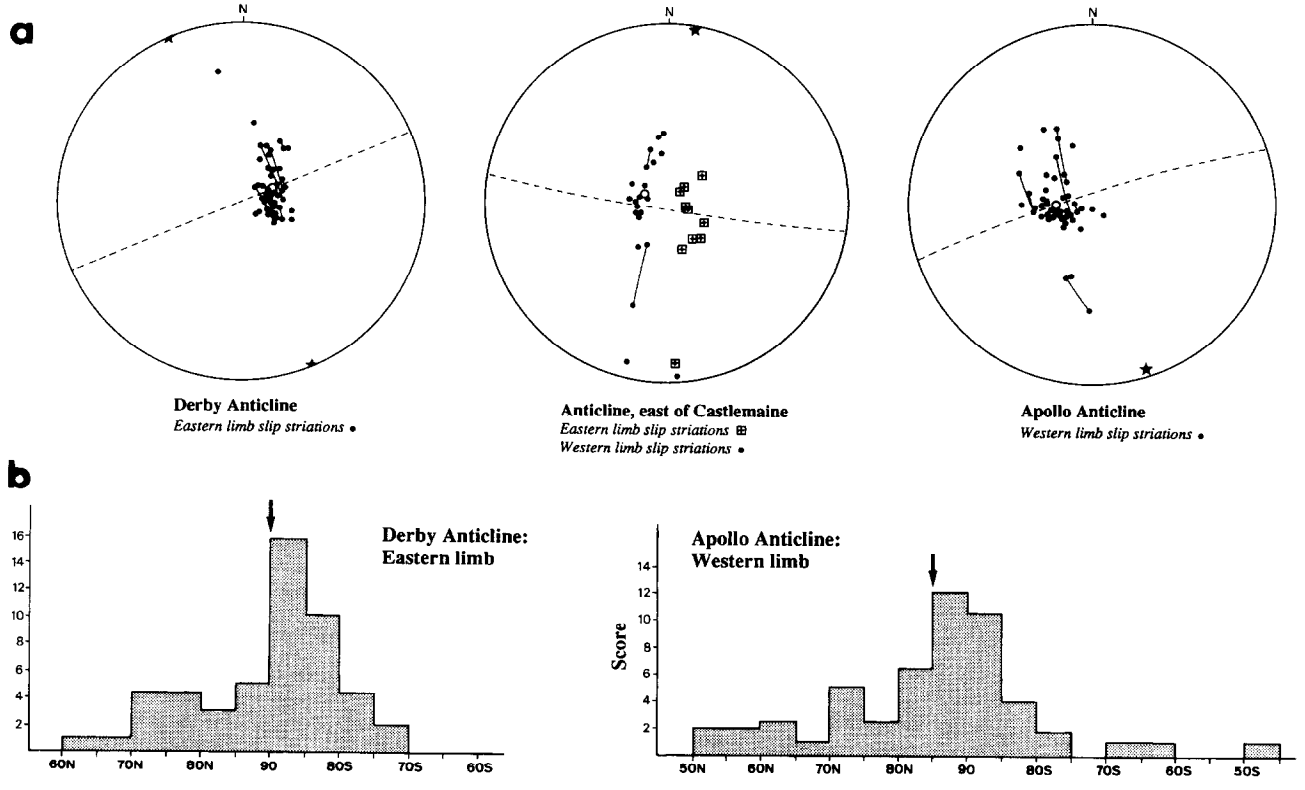

Fig. 5. (a) Stereographic projection (Schmidt net) of slip-lineation data (dots and boxed crosses) with mean lineation orientation shown as an open circle. Note that the mean lineation orientation for the anticline east of Castlemaine, refers only to the data from the western limb. Calculated local fold hinge orientations are represented by stars. Lineations measured on the same laminated vein are connected by great circle arcs on these nets. The broken great circle represents the girdle of best fit of poles to beds (which was used to calculate the mean fold-axis orientation). Derby Anticline (location B, Fig. 1), anticline east of Castlemaine (location E, Fig. 1), Apollo Anticline (location D, Fig. 1). (b) Histograms of 5° pitch class intervals for slip lineations measured on bedding slip planes for two of the surveyed fold limbs. The arrow represents the mean lineation

the Derby Anticline a commonly recurring pattern of lineation orientations was noted such that the slip lineations on vein footwalls lie consistently 20–40° clockwise of slip lineations on the vein hangingwall (viewed towards the west). The significance of this pattern is unclear but is suggestive of a growth sense for the veins either by accretion consistently at the hangingwall contact or consistently at the footwall contact, as was concluded for similar veins from Hill End, New South Wales by Windh (1989).

A histogram showing the distribution of slip-lineation pitches for data from the Derby and Apollo Anticlines is presented in Fig. 5(b). In both examples the distributions appear to represent roughly normal populations with the modal pitch class interval coinciding with the mean for the pitch data. There is a possibility of more than one population of pitches in the measurements. The results further support the relationship between the slip lineations and flexural-slip folding.

Thickness variations of laminated veins

The statistics for laminated vein thicknesses from this study and from a survey of available mine sections is presented in Table 4. Jessell *et al.* (1994) did not quote thicknesses of the laminated veins apart from noting that 'Type I' veins (representing a microstructure characterized by repetitive stepping of inclusion trails, and accounting for about 10% of all bedding-parallel veins) were 50–100 mm thick and 'Type II' veins (the remaining 90% of veins with rough wallrock seams, and lacking the Type I microstructure) were generally less than 200 mm thick. Fowler (1996) has concluded that the majority of veins of both these 'types' formed during the folding process. Therefore, they will not be treated as separate data populations here.

From Table 4 it is clear that the mean laminated vein thickness from surface exposures is much lower than that determined from mine sections, supporting the suggestion above that thinner bedding-parallel veins were systematically overlooked during underground surveys. The histogram for vein thickness (Fig. 6) shows that more than half of the observed vein thickness measurements are less than 10 mm. Greater thicknesses are consistently less frequent.

Table 4. Thickness of bedding-parallel laminated veins

	Range mean T* (mm)	Mean T† (mm)
This study	12–34	19‡
Mine sections	11–131	62

*'Range mean T' refers to the range of mean thickness measurements for laminated veins (in mm) from each section.

†'Mean T' is the mean vein thickness (in mm) for all the data.

‡One outstandingly thick vein of 220 mm had a significant effect on the data mean. Ignoring this single vein, the overall mean laminated vein thickness is 17 mm, and the range of mean thicknesses is 12–25 mm.

Inspection of laminated veins along strike and dip indicates that individual veins vary in thickness variations. Thick laminated veins are known to taper towards their edges (Keppie, 1976; Mawer, 1987; Wilkinson, 1988). Jessell *et al.* (1994) noted a pronounced lensing of laminated veins along strike at Little Bendigo, Castlemaine. In general, laminated vein thicknesses vary smoothly. Taken in isolation, the histogram in Fig. 6 could represent either: (a) random measurements of tapering veins which are essentially similar to each other in dimensions; or (b) random thickness sampling of veins with a range of dimensions. Tanner (1989) noted a relationship between bedding-parallel vein thickness and net slip across the vein walls. Thus vein thickness variations interpreted as (b) above have implications for bedding slip-plane activity during folding. Further discussion on this problem is presented below.

Lateral continuity of laminated veins

Despite generally inadequate surface outcrop away from railway cuttings, the continuity of bedding slip

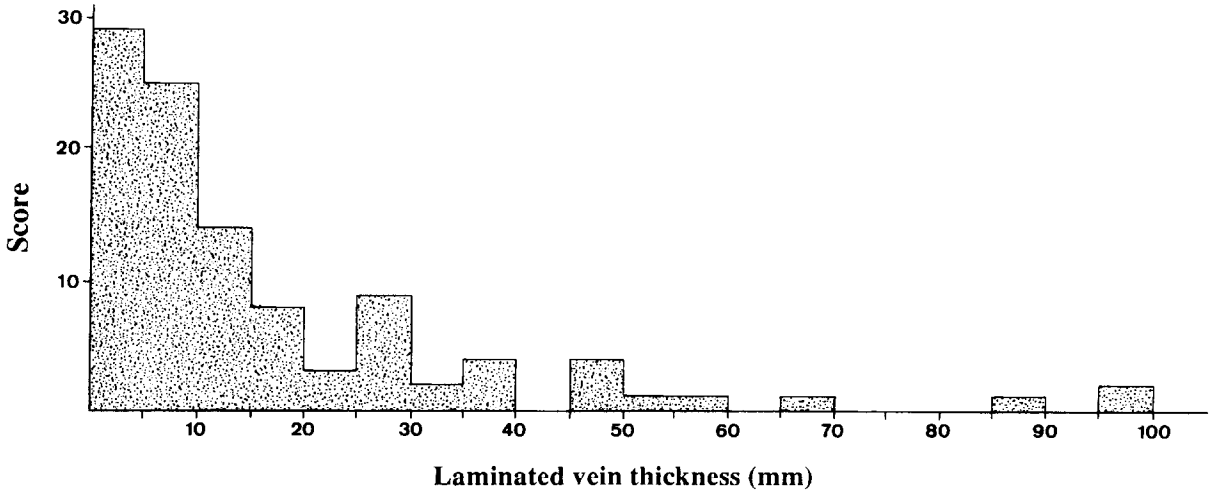

Fig. 6. Histogram of 5 mm laminated vein thickness class intervals for data from all measured sections.

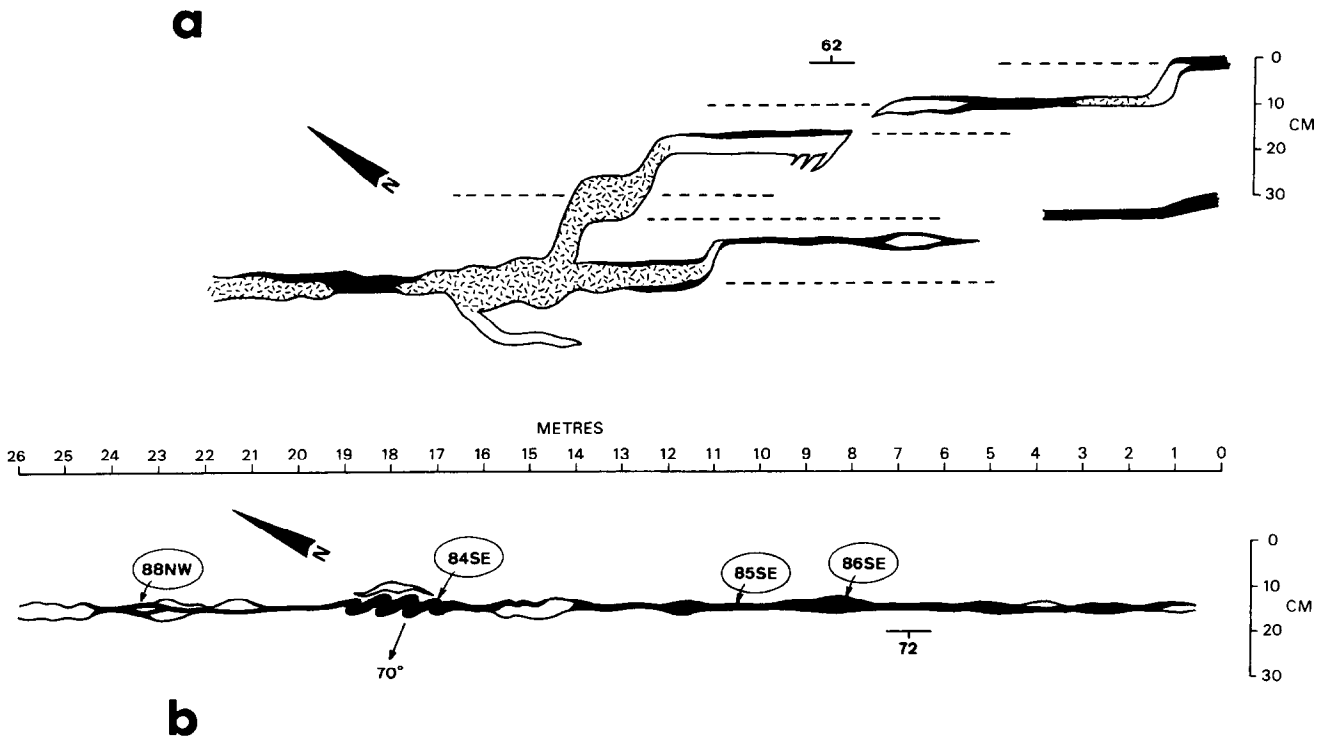

Fig. 7. Map sketches of some of the compositional and geometric characteristics of laminated bedding-parallel veins from the Bendigo–Castlemaine goldfields. Black areas are laminated vein quartz, unornamented areas are massive vein quartz (sometimes vuggy) and random-dashed areas are limonite-cemented vein-quartz breccia zones. (a) From the eastern limb of the New Chum Anticline, Victoria Hill (location C, Fig. 1), showing transfer of bedding-parallel veins from one stratigraphic level to another. Also lensing and branching of veins. (b) From the western limb of the Apollo Anticline (location D. Fig. 1) showing lensing, mesoscopic folding and consistency of slip-lineation orientation on vein walls over considerable strike distances. The pitches of footwall slip lineations are circled. The trend and plunge of small-scale folds in the laminated veins are represented by an arrow and number.

surfaces was investigated in three ways: (a) direct measurements of continuity in areas of continuous outcrop; (b) correlation of slip horizons from one fold limb to the other across a fold hinge, using surface data from railway cuttings; and (c) measurements of the extent of slip planes in mine sections.

Direct measurements of bedding slip-plane continuity. The eastern limb of the New Chum Anticline at Victoria Hill, and sluiced areas of the western limb of the Apollo Anticline at White Hills (Fig. 1, locations C and D) are amongst the few areas where continuous outcrop is sufficient for the strike continuity of laminated veins to be directly measured. Laminated veins which reached a maximum observed thickness of a few millimetres could be traced only for a few metres along strike and disappear down-dip over a distance of a few metres. The strike extent of laminated veins that reach a few centimetres in maximum thickness was measured as several tens of metres, up to about 100 m. Outcrop did not allow for the determination of the strike extent of veins with thicknesses up to tens of centimetres.

Sketches showing bedded vein thickness variations and other characteristics along strike are shown in Fig. 7. Lensing and complex interlacing of laminated vein quartz, massive vein and vuggy quartz, and limonite-cemented brecciated vein quartz and siltstone particles are observed along the strike of individual veins. A full description of the characteristics of these veins along strike is beyond the scope of this paper; however one interesting feature worthy of note is the frequent bifurcation of the veins. The veins usually rejoin to enclose a lens of complexly folded siltstone, however if the two branches of the vein are separated by about 15 cm or more, one branch usually splays off to become a new slip horizon (Fig. 7a). Veins also ramp to new stratigraphic levels via non-laminated dilation zones or zones of brecciated vein quartz (Fig. 7a). We strongly suspect that this is one origin of the pairing or clustering of slip planes described by the vein spacing data. Another feature worthy of note is the asymmetric parasitic folding of some sections of the laminated veins (e.g. between 15 and 19 m in Fig. 7b). Some of the latter fold hinges are truncated by later laminae and earlier-formed fibre lineations may be folded as described by Jessell *et al.* (1994). At least in some cases, the folding is spatially related to sedimentary discontinuities in the slip plane due to truncation or thinning of the siltstone host by an overlying sandstone bed.

Correlation of bedding slip planes around fold hinge zones. In only one surface stratigraphic section was

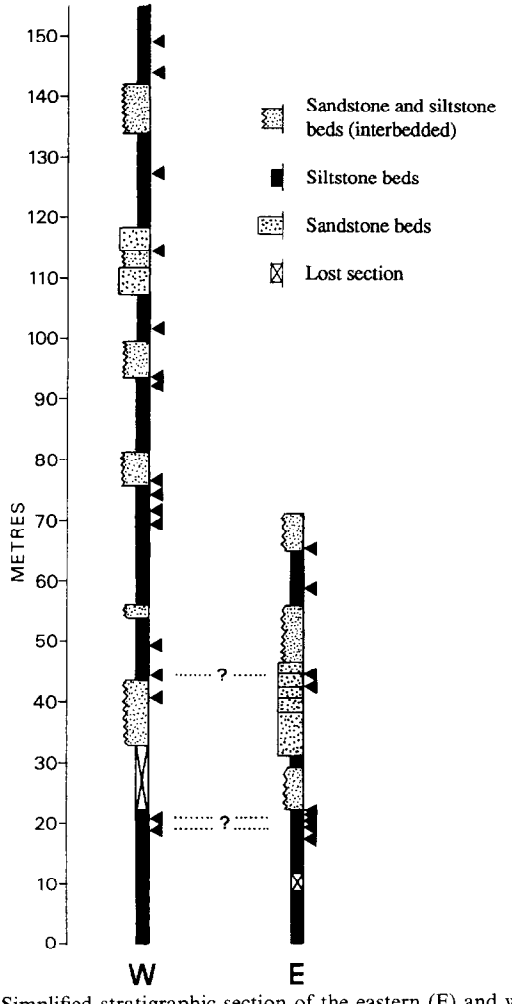

Fig. 8. Simplified stratigraphic section of the eastern (E) and western (W) limbs of the unnamed anticline in the Castlemaine railway cutting (location E, Fig. 1), demonstrating the problematic correlation of bedding slip planes from one limb to the other across the hinge.

continuity of outcrop sufficient on both limbs of a fold to test the continuity of bedding slip planes across a fold hinge. Simplified stratigraphic sections with locations of movement horizons for the east and west limbs of the Castlemaine fold (Fig. 1, location E) are shown in Fig. 8. In general, correlation of slip planes from limb to limb is not successful, although the horizons at stratigraphic height 44 m on the western limb and at 45 m on the eastern limb are both 30 cm thick and apparently correlate. If they do, then this 30 cm thick laminated vein extends for at least 254 m.

Extent of bedding slip planes in mine sections. The continuity of veins around fold hinge zones as seen in mine sections is apparently much more frequent than observed in the surface sections. Unfortunately there are few examples where underground workings extended far enough in the direction normal to the axial plane of the main anticline to give an indication of the extent of the laminated veins ('backs') along the dip direction. In general, laminated veins which reach 10 cm in thickness extended for at least a few hundred metres. The most extensive vein (with available thickness data) was a 23 cm thick vein from the Little '180' Mine, which was continuous over the hinge of an anticline for a distance of 530 m. It appears that most of the laminated veins that are 10 cm or more in thickness are traceable across anticlinal and sometimes synclinal hinges from one limb to the next.

In conclusion, the average extent of millimetre-thick bedding-parallel veins is measured in metres; the extent of veins reaching a few centimetres thick is several tens of metres; whilst the extent of veins that reach tens of cms in thickness is several hundreds of metres. The length of faults is known to bear a direct, possibly linear, relationship with maximum fault displacement (Elliott, 1976; Watterson, 1986; Clarke and Cox, 1996). The correlation of laminated vein thickness with extent of slip planes supports such a relationship between vein thickness and net slip.

Relations between laminated vein thickness, vein spacing and stratigraphic position

The mean spacing of bedding slip planes and mean laminated vein thicknesses for each of the five fold limbs measured are presented in Table 5, in order of increasing mean spacing. There is an overall trend of increasing mean laminated vein thickness as the spacing of bedding slip planes increases. Since the net slip on the bedding slip planes may be expected to increase as the spacing of slip planes increases (Ramsay, 1967), this result is in accord with a sympathetic relationship between laminated vein thickness and net slip. Interestingly, the largest mean spacings occurred on western limbs of anticlines. Since the number of anticlines examined in this study is small, we are uncertain of the significance of this observation.

The laminated vein/bedding slip-plane spacing and vein thickness attributes are shown in Fig. 9 for all the data. This was intended to determine whether the sympathetic increase in mean laminated vein thickness with increasing mean vein spacing described above was evident for data from individual veins. Individual vein thicknesses plotted against stratigraphic distance to the nearest slip plane above the vein are shown in Fig. 9(a). There is no obvious correlation, either for the whole

Table 5. Mean bedding slip-plane spacing and laminated vein thickness data

	Mean spacing (m)	Mean T (mm)
Eastern limb Derby	5.1	13.1
Eastern limb Castlemaine	6.7	11.3
Eastern limb New Chum	8.1	12.4*
Western limb Castlemaine	11.0	18.5
Western limb Garden Gully	11.1	18.3*
Western limb Apollo	11.7	25.0

*Both values neglect a single outstandingly thick vein which would strongly influence the mean, if included.

dataset or for data groups from each fold limb. The concentration of data points near the origin reflects the abundance of thin laminated veins and the tendency for veins to occur in close-spaced clusters. The graphs of vein thickness vs the stratigraphic distance to the nearest slip plane below, or the nearest slip plane (above or below), are not presented but do not produce any correlations.

A graph of vein thicknesses vs the thickness of the nearest laminated vein is shown in Fig. 9(b). Apart from a clustering of data points near the origin (for the same reasons described above), there is no evident co-dependence. The thickness of veins vs their estimated along-limb distance from the fold hinge is shown in Fig. 9(c). There is a tendency for laminated veins, especially thin ones, to be more abundant in the first 150 m. This was noted by Fowler and Winsor (1992), although the contribution to this pattern is mainly from data of the Derby and New Chum Anticlines, Bendigo. There is no equivalent tendency for veins to become abundant or thicker as the axial plane of a syncline is approached (typically located at a distance of 400–450 m).

DISCUSSION

There is clearly an abundance of thin flexural-slip-related laminated veins on the limbs of the chevron folds in the Bendigo–Castlemaine goldfields that have previously escaped attention in subsurface mine surveys. This may have been due to the poor underground lighting conditions which existed in the early part of this century, when the mines were surveyed. Unfortunately, almost all of the mines are now inaccessible. The thinnest veins (less than 2 cm) form the majority of the bedding slip-plane populations in all of the sections studied in this region. A comparison of the mean spacing of bedding slip planes determined for the Bendigo–Castlemaine region with those reported from other studies is shown in Table 6. The mean spacing for bedding slip planes in the Bendigo–Castlemaine region lies between the extremes of reported values, and is amongst the wider spaced examples. The differences in average spacing of slip planes among the localities listed in Table 6 are not obviously accounted for by systematic differences in fold tightness or bed thickness.

Table 6. Comparison of mean bedding slip-plane spacing of the Bendigo–Castlemaine region with that of other areas

	Mean spacing range (m)
Chappell and Spang (1974)	0.15–0.3
Borradaile (1977)	0.5–0.7
Kölbel (1940)	0.5–0.7
Tanner (1989)	0.2–1.2
Cloos and Martin (1932)	0.2–2.0
Kenny (1936)	0.8–13
This study	3.5–11.7
Johnson and Page (1976)	30–43

The data on slip-plane spacing and laminated vein thickness variations may be used to test some ideas on the activity of the flexural-slip mechanism during folding. First, let us return to an earlier hypothesis that the laminated veins may be essentially equidimensional. This would imply that the thinnest veins simply represent the thinner parts (e.g. peripheries) of thicker veins. The thinner vein margins would form by distal propagation of the active slip area over the bedding plane, hence we may still expect a relationship between vein thickness and magnitude of slip displacement. Also, there would be a relationship between the continuity of the vein and its thickness, as observed. Such a population of veins of similar dimensions may have roughly uniform values of maximum net slip, and the simplest interpretation of the latter would be that the slip planes were slip-active simultaneously. However, the vein thickness data (Fig. 6), at least, is inconsistent with such a model. The thick laminated veins exposed in subsurface sections show gradual thinning down-dip away from fold hinges. The histogram in Fig. 6 shows that those class intervals representing the thinnest veins contain the majority of the data. If a significant proportion of thin veins were lateral extensions of thick veins then there should be far more of the intermediate thickness veins than are found. The distribution of thicknesses is suggestive of a significant population of thin veins, some of which may be lateral extensions of thicker veins.

The possibility that all of the slip planes are active over approximately the same time interval is also inconsistent with the data. Although there is a statistical relationship between mean laminated vein thickness and mean slip-plane spacing, as seen in Table 5, this is not seen in the plot of individual vein thickness against distance to nearest slip plane above (Fig. 9a), nor in the plot of vein thickness against thickness of nearest-neighbour laminated vein (Fig. 9b). Since the amount of slip at any constant limb dip is proportional to the spacing between slip planes (Ramsay, 1967), a relationship between net slip (hence vein thickness) and spacing would be expected for individual laminated veins if they had been simultaneously active.

Tanner (1989) speculated upon the progressive development of slip planes with increasing fold limb dip (or rather with decreasing interlimb angle), presumably on the basis that measured slip-plane spacings decreased as limb dips increased. Most workers have assumed (mainly for simplicity) that bedding slip was active throughout folding and occurred on evenly spaced bedding planes, although Chappell and Spang (1974) comment on the possibility of variable activity of bedding slip planes during folding, and noted also the physical discontinuity of slip planes as a probable contributor to local strain inhomogeneities in folded layers. Fowler and Winsor (1996) also suggested intermittent stick–slip activity on the limbs of chevron folds evolving from box folds, the activity being controlled by hinge migration rates.

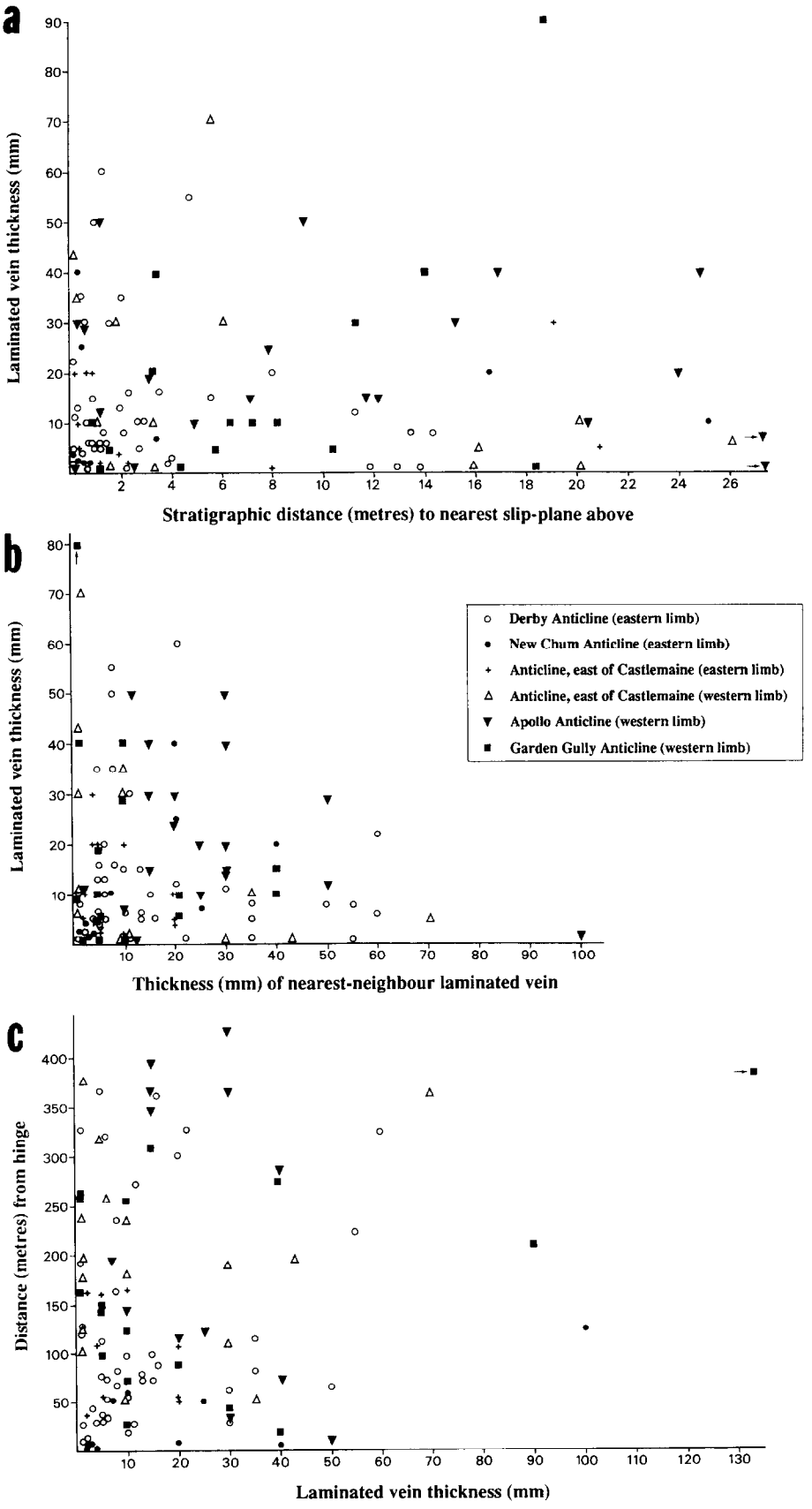

Fig. 9. (a) Individual laminated vein thickness plotted against stratigraphic distance to the nearest slip plane above the vein (data from all sections). (b) Plot of laminated vein thickness vs the thickness of the nearest laminated vein (data from all sections). (c) Plot of the thickness of veins vs their calculated distance (along the limb) from the fold hinge (data from all sections). See text for discussion.

Table 7. Parameters used in the computer simulation of slip-plane generation

A	fold limb dip (radians)
t_1	competent layer thickness
t_2	incompetent layer thickness
η_1	viscosity of the competent layer
η_2	viscosity of the incompetent layer
$\dot{\gamma}'_1$	internal shear strain rate for the competent layer
$\dot{\gamma}'_2$	internal shear strain rate for the incompetent layer
Γ	the ratio $\dot{\gamma}_1/\dot{\gamma}_2$
μ	coefficient of internal friction for the competent–incompetent layer contacts
s	magnitude of the net slip on a slip plane
T	thickness of the slip-plane-free packet of beds (or 'welded' packet) above a slip plane
τ_m	material shear-strength constant for the competent–incompetent layer contacts
τ	shear stress on the competent–incompetent layer contacts
σ'_1, σ'_3	maximum and minimum effective principal stresses
σ'	effective normal stress on the competent–incompetent layer contacts
λ	the ratio of fluid pressure/σ_3

Computer simulation of progressive generation of layer slip planes in a steepening fold limb

In order to investigate the slip-plane spacing and bedding-parallel laminated vein thickness relations which result from progressive initiation of new slip planes during fold limb steepening, a simple computer model was devised as described below. Parameters used in this program are summarized in Table 7.

Experimental multilayer. A multilayer sequence of alternating constant thickness (t_1) competent layers and randomly ordered incompetent layer thicknesses (t_2) was generated by computer as explained below. The frequency distribution of the incompetent layer thicknesses matched those of the siltstone beds in the Bendigo–Castlemaine region as shown in Fig. 4(a). The competent layers all have the average thickness of sandstone beds in the Bendigo–Castlemaine region (0.6 m) as determined from the detailed measured stratigraphic sections. Four hundred such incompetent–competent layer pairs with the above frequency distribution were randomly stacked. This number allows for a multilayer stack with approximately the same total thickness as the cumulative measured sections in the Bendigo–Castlemaine region. This stacking procedure represents minimal stratigraphic duplication of the local stratigraphy since the data sections include a broad range of stratigraphic levels (Table 1).

Condition for the initiation of slip planes in this multilayer model. There are several possible triggers for the initiation of slip along bedding planes during folding. These include stress controls: (a) when the material shear strength of the layer contacts is exceeded as shear stresses rise (brittle shear behaviour, normal stress dependent); or (b) when effective stresses on bedding planes are reduced by elevated pore fluid pressures (Johnson and Page, 1976; Cosgrove, 1993); or (c) when a critical shear stress value is reached (plastic behaviour, normal stress independent) (Chappell and Spang, 1974), or *shear strain rate controls*; or (d) when a viscous resistance to slip is overcome (Chappell and Spang, 1974; Cruikshank and Johnson, 1993; Treagus, 1993). Ramsay (1974) investigated the stress, strain and strain rates found on chevron fold limbs in alternating competent–incompetent multilayers. His model presumed welded interlayer contacts, and predicted that the ratio of competent layer to incompetent layer shear strain rates (i.e. $\Gamma = \dot{\gamma}_1/\dot{\gamma}_2$), was a function of t_1/t_2 and limb dip A. Ramsay noted that this result is incompatible with the model assuming welded interlayer contacts, because along the welded contacts a single shear stress value τ should exist at the interface, and therefore Γ should have a constant value related only to the relative viscosities of the layers which share the interface (i.e. Γ should equal η_2/η_1). To resolve this inconsistency Ramsay proposed *inter alia* that where the calculated value of Γ at any limb dip differed from η_2/η_1, shear stress in the competent or incompetent layer would be resisted sufficiently to allow Γ to remain constant. However, this requires the layer interfaces to resist rapidly rising excess shear stresses, especially in the thinner incompetent layers, as limb dip increases. We have used a simple Coulomb criterion to model shear failure along a competent–incompetent layer interface, when the total shear stress (τ) at the interface exceeds $\tau_m + \sigma'\mu$ (where τ_m is a material shear-strength constant (at zero normal stress), σ' is the effective normal stress on the contact and μ is the coefficient of internal friction). We have used this criterion to investigate the generation of bedding-parallel slip planes in our model.

Since we do not know the actual values for η_1 and η_2, we have opted for an intermediate value of η_2/η_1 of 1/10, and a value for μ of 0.3 (Ibanez and Kronenberg, 1993). τ_m was experimentally varied as described below. Γ and τ were calculated using equations (22) and (18) of Ramsay (1974): $\Gamma = [(t_1/t_2 + 1)\sec^2 A - t_1/t_2)]^{-1}$ and $\tau = (\sigma'_1 - \sigma'_3)\sin(A)\cos(A)$, and normal shear stress on layer $\sigma' = (\sigma'_1 + \sigma'_3)/2 - (\sigma'_1 - \sigma'_3)\cos(2A)/2$. σ'_3 was assigned a value of 7 MPa and was allowed to increase as limb dip steepened, reflecting constant loading. σ'_1 was set at 47 MPa, and both constant normal stress

and constant loading situations were explored. These initial effective stress values were chosen on the basis of confining pressure being about 150 MPa; fluid pressure/σ_3 (λ) being 0.95 (Price and Cosgrove, 1990); and stress difference ($\sigma'_1 - \sigma'_3$) being about 40 MPa (Etheridge, 1983).

Calculation of net slip on slip planes. Our model considers the simple situation of a planar limb of a chevron fold (or box fold) rotating about the hinge during limb steepening. Limb dip (A) was increased by increments of 1°. At each increment Γ and τ (as functions of A) were calculated and the difference between Γ and η_2/η_1 expressed as additional shear stress ($\delta\tau$) on the contact. Both components of shear stress τ and $\delta\tau$ act on the same surface area and in the same direction so may be added. At each increment of limb dip the value $(\tau + \delta\tau)$ was compared to $\tau_m + \sigma'\mu$. If $(\tau + \delta\tau) \geq \tau_m + \sigma\mu$ for any contact between a competent and incompetent bed, a slip plane was set at that contact and the multilayer was divided into two packets of layers at that horizon. As dip was gradually increased the increment of slip (δs) on any slip plane was calculated according to the formula $\delta s = T(\tan(A) - \tan(A - \pi/180) - \pi/180)$ (adapted from Ramsay (1967, equation 7-39), and where A is here expressed as radians), and T is the thickness of the packet of overlying beds during that increment of dip. The value of δs was then added to the net slip on the slip plane. The limb dip was increased in 1° increments up to 75°. At each stage the shear stress on existing slip planes was also tested to determine whether slip would continue on these planes (on the basis of τ exceeding $\sigma'\mu$).

Experimental variation of model parameters to obtain the observed mean slip-plane spacing. The value of τ_m was varied until a mean slip-plane spacing of 8.9 m was obtained for the multilayer. The value of τ_m obtained was 3 MPa.

Results of the computer simulation

Using the above model a graph of net slip vs stratigraphic distance to the nearest slip plane above, for each slip plane, is presented in Fig. 10(a). For the same data, the plot of net slip vs net slip of the nearest slip plane is shown in Fig. 10(b). Considering the rough correspondence of vein thickness to net slip, Fig. 10(a & b) is to be compared with Fig. 9(a & b), respectively. As with Fig. 9, there are no obvious correlations between any pair of variables in Fig. 10. In both Figs 9 and 10 there is a preponderance of thin veins (and corresponding slip planes of low (< 10 m) net slip). Although simplistic, the computer model gives an explanation for the lack of correspondence between laminated vein thickness and slip-plane spacing, despite the evident flexural-slip origin of the veins, namely that the net slip on any slip plane results from the addition of many smaller slip increments whose individual magnitude is determined by the ever-

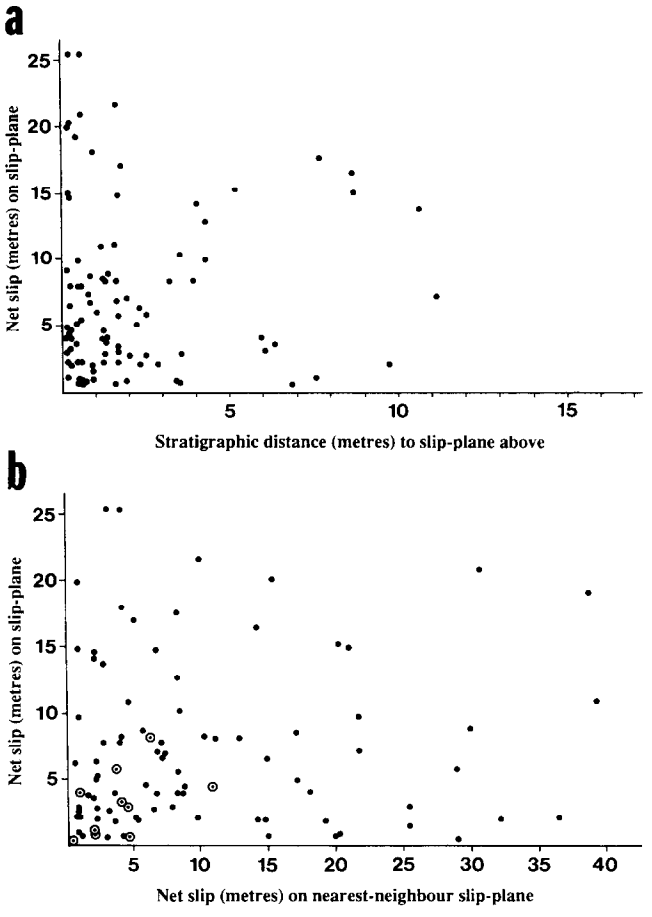

Fig. 10. Data derived from a computer model for the generation of slip planes in the Bendigo–Castlemaine goldfields (see text for the rationale of the model and the parameters used). (a) Plot of net slip vs stratigraphic distance to the nearest slip plane above. (b) Plot of net slip on a slip plane vs net slip of the nearest slip plane. Circled dots represent data for slip planes which formed after a 60° limb dip.

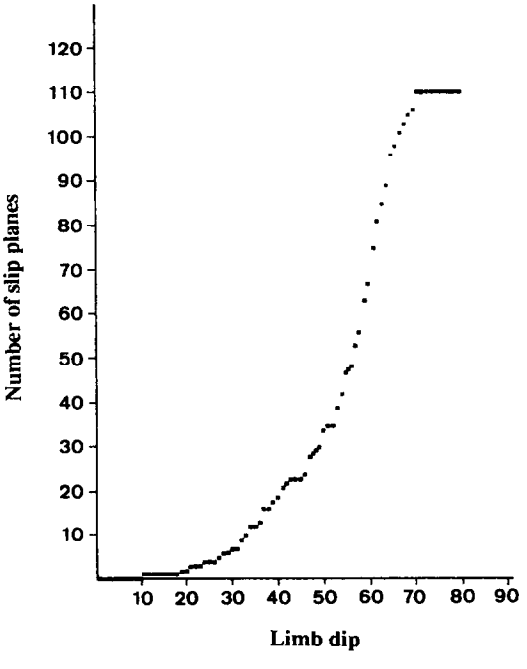

Fig. 11. Graph of the number of active slip planes vs limb dip for data derived from a computer model for the generation of slip planes in the Bendigo–Castlemaine goldfields (see text for the rationale of the model and the parameters used).

changing thickness of slip-free layer packages above the slip plane. The history of change of thickness of these packages is determined by the (randomly-determined) order of stacking of the incompetent layers. In accord with the latter, our model demonstrated no apparent regularity in the stratigraphic location of slip planes as they progressively formed.

A graph of the cumulative number of slip planes generated as limb dip increases for a typical run of this program is shown in Fig. 11. Slip planes first appeared at low limb dips (typically 10–20°) and rapidly increased in number to limb dips of about 70°. This is quite different to the results of Dubey and Cobbold (1977) and Behzadi and Dubey (1980), which were based on Plasticine multilayer experiments with lubricated layer interfaces, where the greatest slip activity occurred between limb dips of 30° and 50°. Behzadi and Dubey (1980) also observed that interlayer slip activity ceased by limb dips of 65°. De Sitter (1958) and Ramsay (1967) assumed frictionless layer interfaces and judged that interlayer slip activity would cease as layer-parallel shear stresses declined, by the stage that limb dips of about 60° were attained. The computer model was explored by varying values of σ'_1 and σ'_3, and considering constant σ'_1 or constant loading, and varying values of τ_m and μ and η_2/η_1, but no combination of these (restricted to generating a mean slip-plane spacing of 8.9 m) resulted in cessation of the generation of new slip planes at 65° limb dip. All combinations of these parameters yielded populations of slip planes dominated by those with low values of net slip (e.g. the slip planes generated between 60° and 70° and are circled in Fig. 10b). These results argue against the presumption in earlier models of simultaneously active, uniformly spaced slip planes, and also suggest that the importance of flexural slip will vary during fold growth.

Limitations of the computer model

We have chosen a multilayer with Newtonian viscous properties (mainly for simplicity), although it has been suggested that power-law viscous properties may be a prerequisite for the formation of chevron styles in single layers and multilayers (Cruikshank and Johnson, 1993; Hudleston and Lan, 1994). For power-law viscous multilayers the competent to incompetent layer viscosity ratio increases dramatically as limb dip increases (Treagus, 1993), at least for the case where the stress exponent is the same for both layers. This leads to spectacular changes in strain rates in the competent layers, while flow in the incompetent layers remains relatively unchanged by values of the stress exponent but are affected more by incompetent layer relative thickness (Treagus, 1993). We have found it impossible to achieve mean slip-plane spacings similar to those found at Bendigo–Castlemaine using viscosity ratios greater than 10 in order of magnitude. At present, there are no power-law viscous layered models which take into consideration the fact that contacts are gradational between sandstones and overlying siltstones in these sequences.

The results of the computer simulation are consistent with the observed dominance of thin, commonly weakly deformed, slip-striated laminated veins in the Bendigo–Castlemaine area, and they suggest that flexural-slip activity may extend over most of the fold amplification history. Gray and Willman (1991) estimated bulk shortening associated with the homogeneous flattening strain component in the Central Victorian chevron-folded thrust sheets (including the Bendigo–Castlemaine region) to be about 40%, from which, after unstraining, they restored the folds to a shape approximating their form due to the buckling shortening component only. The unstrained folds had an average 89° interlimb angle (corresponding to about 45° limb dip). Yang and Gray (1994) further suggested that strain in these folded sandstone beds was too low for the folds to have formed by buckle folding followed by homogeneous flattening, and suggested that some minor bedding slip accompanied limb rotation (but only up to limb dips of 60°) during cleavage development. They argued that the coaxial strain history, indicated by straight pressure shadows around pyrite porphyroblasts in the slates, argued against flexural flow in the slates (although not against flexural slip) accompanying cleavage-related shortening strains. Cosgrove (1995) concluded that bedding-plane slip during folding was thought to precede cleavage formation. Our computer model suggests that flexural-slip activity was continuing well into this stage of homogeneous flattening. Fowler (1996) concluded that most of the laminated veins from this region had formed during or after crenulation cleavage development (which is the first tectonic foliation; White and Johnston, 1981) in the slates, that is during the homogeneous flattening stage of the chevron folds. This conclusion was based on bedding-parallel vein microstructures (Type I) which showed phyllosilicate inclusion traces formed by detachment of syntaxial overgrowths on prominent crenulation cleavage phyllosilicate domains in the vein wall. Therefore it may be necessary, in models which explore flexural-slip activity and stress distributions on the limbs of developing chevron folds, to consider the effects of pressure-solution shortening on the magnitude of σ'_1.

CONCLUSIONS

Bedding slip planes and associated slip-striated laminated quartz veins developed during flexural-slip folding of alternating sandstone and siltstone beds in the Bendigo–Castlemaine goldfields, southeastern Australia. Slip-plane and laminated-vein data from surface sections, representing the limbs of five major anticlines, suggest a mean spacing of bedding slip planes of 8.9 m or less, and a mean thickness of laminated veins of 19 mm. These values are significantly lower than values (13.0 m

and 62 mm, respectively) obtained from underground mine section surveys, suggesting that the narrower, less conspicuous, bedded veins were consistently overlooked in the latter surveys. More than half of the observed laminated vein thicknesses were less than 10 mm. Bedded veins greater than 100 mm in thickness are commonly traceable from limb to limb across anticlinal hinges, whereas veins thinner than 20 mm (the majority) do not generally have partners on the same stratigraphic horizon across fold hinges. The typical strike extent of millimetre-, centimetre- and decimetre-thick laminated veins is in the order of metres, several tens of metres and several hundreds of metres, respectively.

Sedimentary facies types apparently are not a controlling factor on the location of bedding slip planes. Ninety-two per cent of all the identified bedding slip planes occurred within siltstones or at their contact with overlying sandstones. Bedding slip planes are concentrated in thin siltstones, although the thinnest siltstone beds are under-represented, probably due to the physical discontinuity of these layers. Ramping and bifurcation of veins may explain the tendency of bedding slip planes to occur in close-spaced pairs or groups. Mean slip-lineation orientations lie within 5° (of pitch), and 80–95% of individual lineation pitches lie within 20° (of pitch) of being orthogonal to the local fold axis.

The mean laminated vein thicknesses for individual fold limbs increases as the mean spacing of bedding slip planes increases, supporting the suggestion by Tanner (1989) that there is a positive correlation between laminated vein thickness and net slip for laminated veins. The latter relationship is not observed when individual vein thicknesses are plotted against stratigraphic distance to the nearest neighbour slip plane above (or below, or overall). The vein thickness data and the lack of correlation of individual vein thickness with stratigraphic distance to the nearest-neighbour slip plane do not favour a model in which the slip planes are roughly equidimensional and roughly contemporary in their slip activity.

The generation of slip planes was modelled by computer for a multilayer sequence of alternating competent and incompetent layers, with the former having constant thickness, and the latter having the same thickness frequency distribution as those measured in the Bendigo–Castlemaine surface sections. Using this model, the progressive formation of new interlayer slip planes during limb steepening was explored. Slip-plane formation was considered to be triggered by the increasing shear strain rate incompatibilities between competent and incompetent layers during limb steepening, expressed as increased shear stresses overwhelming finite shear strength and friction on layer contacts. The net slip on each slip plane was monitored during limb steepening. Model parameters were adjusted to yield an average slip-plane spacing similar to that observed in the Bendigo–Castlemaine region. This resulted in a population of slip planes dominated by low net slip (< 10 m net slip) slip planes (probably corresponding to the thin discontinuous laminated veins), with slip-plane generation occurring between limb dips of 10° and 70°. The continuity of slip-plane activity to such high dips suggests that flexural slip has accompanied homogeneous flattening of the folds. This conclusion is in accord with the microstructures of laminated veins of the region which indicate that these veins formed during or after crenulation cleavage development in the slate wallrocks.

Acknowledgements—The authors would like to acknowledge the constructive suggestions and questions by Dave Gray and Geoff Tanner in reviewing this paper, and the thoughtful comments by Peter Hudleston.

REFERENCES

Behzadi, H. and Dubey, A. K. (1980) Variations of interlayer slip in space and time during flexural folding. *Journal of Structural Geology* **2**, 453–457.

Borradaile, G. J. (1977) On cleavage and strain: results of a study in West Germany using tectonically deformed sand dykes. *Journal of the Geological Society of London* **133**, 146–164.

Boulter, C. A. (1979) On the production of two inclined cleavages during a single folding event; Stirling Range, S.W. Australia. *Journal of Structural Geology* **1**, 207–219.

Bucher, M., Foster, D. A. and Gray, D. R. (1996) Timing of cleavage development in the western Lachlan Fold Belt: new constraints from Ar^{40}/Ar^{39} geochronology. *Geological Society of Australia Abstracts* **41**, 66.

Cas, R. A. F., Cox, S. F., Bieser, L., Clifford, B. E., Hammond, R. L., McNamara, G. and Stewart, I. (1983) Lower Ordovician turbidites of central Victoria: submarine fan or basin plain, and tectonic significance. *Geological Society of Australia Abstracts* **9**, 200–201.

Chappell, W. M. and Spang, J. H. (1974) Significance of layer-parallel slip during folding of layered sedimentary rocks. *Bulletin of the Geological Society of America* **85**, 1523–1534.

Clarke, R. M. and Cox, S. J. D. (1996) A modern regression approach to determining fault displacement–length scaling relationships. *Journal of Structural Geology* **18**, 147–152.

Cloos, H. and Martin, H. (1932) Der gang einer Falte. *Fortschritte Geologie und Palaeontologie Berlin* **11**, 74.

Cobbold, P. R., Cosgrove, J. W. and Summers, J. M. (1971) Development of internal structures in deformed anisotropic rocks. *Tectonophysics* **12**, 23–53.

Cosgrove, J. W. (1993) The interplay between fluids, folds and thrusts during the deformation of a sedimentary succession. *Journal of Structural Geology* **15**, 491–500.

Cosgrove, J. W. (1995) The interplay between fluids, folds and thrusts during the deformation of a sedimentary succession: Reply. *Journal of Structural Geology* **17**, 1479–1480.

Cox, S. F. (1987) Antitaxial crack-seal vein microstructures and their relationship to displacement paths. *Journal of Structural Geology* **9**, 779–787.

Cox, S. F., Etheridge, M. A., Cas, R. A. F. and Clifford, B. A. (1991) Deformational style of the Castlemaine area, Bendigo–Ballarat Zone: implications for evolution of crustal structure in central Victoria. *Australia Journal of Earth Sciences* **38**, 151–170.

Cruikshank, K. M. and Johnson, A. M. (1993) High-amplitude folding of linear-viscous multilayers. *Journal of Structural Geology* **15**, 79–94.

de Sitter, L. U. (1958) Boudins and parasitic folds in relation to cleavage and folding. *Geologie–Mijnbouw* **8**, 277–286.

Dubey, A. K. and Cobbold, P. R. (1977) Non-cylindrical flexural-slip folds in nature and experiment. *Tectonophysics* **38**, 223–239.

Elliott, D. (1976) The energy balance and deformation mechanisms of thrust sheets. *Philosophical Transactions of the Royal Society of London* **A283**, 289–312.

Etheridge, M. A. (1983) Differential stress magnitudes during regional deformation and metamorphism: upper bound imposed by tensile fracturing. *Geology* **11**, 231–234.

Fitches, W. R., Cave, R., Craig, J. and Maltman, A. J. (1986) Early veins as evidence of detachment in the Lower Palaeozoic rocks of the Welsh Basin. *Journal of Structural Geology* **8**, 607–620.

Fowler, T.J. (1996) Flexural-slip generated bedding-parallel veins from central Victoria, Australia. *Journal of Structural Geology* **18**, 1399–1415.

Fowler, T. J. and Winsor, C. N. (1992) The possible role of flexural slip folding mechanism in the development of natural chevron folds from the Bendigo–Castlemaine area, Victoria. *Geological Society of Australia Abstracts* **32**, 227.

Fowler, T. J. and Winsor, C. N. (1996) Evolution of chevron folds by profile shape changes: comparison between multilayer deformation experiments and folds of the Bendigo–Castlemaine goldfields, Australia. *Tectonophysics* **258**, 125–150.

Ghosh, S. K. (1968) Experiments of buckling of multilayers which permit interlayer gliding. *Tectonophysics* **6**, 207–249.

Graves, M. C. and Zentilli, M. (1982) A review of the geology of gold in Nova Scotia. In *Geology of Canadian Gold Deposits*, pp. 233–242. Canadian Institute of Mining and Metallurgy Special Paper **24**.

Gray, D. R. (1988) Structure and tectonics. In *Geology of Victoria*, eds J. G. Douglas and J. A. Ferguson, pp. 1–36. Geological Society of Australia, Melbourne.

Gray, D. R. and Willman, C. E. (1991) Thrust-related strain gradients and thrusting mechanisms in a chevron-folded sequence, southeastern Australia. *Journal of Structural Geology* **13**, 691–710.

Henderson, J. R., Henderson, M. N. and Wright, T. O. (1990) Water-sill hypothesis for the origin of certain veins in the Meguma Group, Nova Scotia, Canada. *Geology* **18**, 654–657.

Hills, E. S. (1972) *Elements of Structural Geology* (2nd edn). Chapman and Hall, London.

Honea, E. and Johnson, A. M. (1976) A theory of concentric, kink, and sinusoidal folding and of monoclinal flexuring of compressible, elastic multilayers. IV: Development of sinusoidal and kink folds in multilayers confined by rigid boundaries. *Tectonophysics* **30**, 197–239.

Hudleston, P. J. and Lan, L. (1994) Rheological controls on the shapes of single-layer folds. *Journal of Structural Geology* **16**, 1007–1021.

Ibanez, W. D. and Kronenberg, A. K. (1993) Experimental deformation of shale: mechanical properties and microstructural indicators of mechanisms. *International Journal of Rock Mechanics & Mining Science and Geomechanics Abstracts* **30**, 723–734.

Jessell, M. W., Willman, C. E. and Gray, D. R. (1994) Bedding-parallel veins and their relationship to folding. *Journal of Structural Geology* **16**, 753–767.

Johnson, A. M. and Honea, E. (1975) A theory of concentric, kink, and sinusoidal folding and of monoclinal flexuring of compressible, elastic multilayers. III: Transition from sinusoidal to concentric-like to chevron folds. *Tectonophysics* **27**, 1–38.

Johnson, A. M. and Page, B. M. (1976) A theory of concentric, kink, and sinusoidal folding and of monoclinal flexuring of compressible, elastic multilayers. VII: Development of folds within Huasna Syncline, San Luis Obispo County, California. *Tectonophysics* **33**, 97–143.

Johnson, A. M. and Pfaff, V. J. (1989) Parallel, similar and constrained folds. *Engineering Geology* **27**, 115–180.

Kenny, J. P. L. (1936) Gold Stairs Mine, Greenborough. *Records of the Geological Survey of Victoria, Australia* **5**(II), 222–223.

Keppie, J. D. (1976) Structural model for the saddle reef and associated gold veins in the Meguma Group, Nova Scotia. *Transactions of the Canadian Institute of Mining and Metallurgy* **69**, 103–116.

Kölbel, H. (1940) über verformung von Kluften bei der Schichtenfaltung am Beispiel des Salzgitterer Sattels. *Geologische Rundschau* **31**, 188–197.

Mawer, C. K. (1987) Mechanics of formation of gold-bearing quartz veins, Nova Scotia, Canada. *Tectonophysics* **135**, 99–119.

Price, N. J. and Cosgrove, J. W. (1990) *Analysis of Geological Structures*. Cambridge University Press, Cambridge.

Ramsay, J. G. (1967) *Folding and Fracturing of Rocks*. McGraw-Hill, New York.

Ramsay, J. G. (1974) Development of chevron folds. *Bulletin of the Geological Society of America* **85**, 1741–1754.

Ramsay, J. G. and Huber, M. I. (1987) *The Techniques of Modern Structural Geology. Vol. 2: Fold and Fractures*. Academic Press, London.

Ramsay, W. R. H. and Willman, C. E. (1988) Economic geology: gold. In *Geology of Victoria*, eds J. G. Douglas and J. A. Ferguson, pp. 454–482. Geological Society of Australia, Melbourne.

Stone, J. B. (1937) The structural environment of the Bendigo Goldfield. *Economic Geology* **32**, 867–895.

Tanner, P. W. G. (1989) The flexural-slip mechanism. *Journal of Structural Geology* **11**, 635–655.

Tanner, P. W. G. (1990) The flexural-slip mechanism: Reply. *Journal of Structural Geology* **12**, 1085–1087.

Tanner, P. W. G. (1992) Morphology and geometry of duplexes formed during flexural-slip folding. *Journal of Structural Geology* **14**, 1173–1192.

Thomas, D. E. (1953) The Bendigo Goldfield. In *Geology of Australian Ore Deposits*, ed. A. B. Edwards, pp. 1011–1027. Fifth Empire Mining and Metallurgical Congress, Australian Institute of Mining and Metallurgy.

Treagus, S. H. (1993) Flow variations in power-law multilayers: implications for competence contrasts in rocks. *Journal of Structural Geology* **15**, 423–434.

Watterson, J. (1986) Fault dimensions, displacements and growth. *Pure and Applied Geophysics* **124**, 365–373.

White, S. H. and Johnston, D. C. (1981) A microstructural and microchemical study of cleavage lamellae in a slate. *Journal of Structural Geology* **4**, 279–290.

Wilkinson, H. E. (1988) Bendigo reef nomenclature. In *Bicentennial Gold '88, Excursion No. 2 Guide: Central Victoria*, pp. 22–27. Geological Survey of Victoria, Australia.

Willman, C. E. (1988) Geology of the Spring Gully 1:10 000 map area, Bendigo Goldfield. Geological Survey Report No. 85. Geological Survey of Victoria, Australia.

Windh, J. (1989) Evidence for gold-bearing quartz vein emplacement during flexural-slip folding, Hill End region, N.S.W. *Geological Society of Australia Abstracts* **24**, 173–174.

Yang, X. and Gray, D. R. (1994) Strain, cleavage and microstructure variations in sandstone: implications for stiff layer behaviour in chevron folding. *Journal of Structural Geology* **16**, 1353–1365.